

NASA TM X-50116

3/p

NA

FACILITY FORM 602

NASA TM X-50116

N65 16923

(ACCESSION NUMBER)

33

(PAGES)

N65 16925

(THRU)

1

(CODE)

(NASA CR OR TMX OR AD NUMBER)

(CATEGORY)

# TECHNICAL M

X-

t: SPACE AND PLANE

(NASA TM X-50116)

auth. Jul. 1963

Presented at the Man  
Technology Confer  
Center, Cleveland, e

Comp

GPO PRICE \$ \_\_\_\_\_

OTS PRICE(S) \$ \_\_\_\_\_

Hard copy (HC) 5.00

Microfiche (MF) 1.50

unc


NAT

WA

## FOREWORD

This document comprises material presented during one session of the Manned Planetary Mission Technology Conference, Lewis Research Center, May 21, 22, and 23, 1963. In order to expedite release to the conferees, the papers are being published with minimum editing and retyping of the original manuscripts. Thus the usual NASA format and style have been compromised.

The purpose of the conference was to explore the possibilities and problems of manned planetary space flight. The results and contemplations of the individual papers should in no sense be regarded as a part of NASA plans and programs. For this reason, the contents of this document are limited for the present to NASA personnel.



## CONTENTS

PARTICLE AND FIELDS IN INTERPLANETARY SPACE by Hugh R. Anderson . . . . .	Page 1 ✓
METEOROID HAZARDS IN NEAR EARTH AND DEEP SPACE by C. T. D'Aiutolo . . . . .	19 ✓

PARTICLE AND FIELDS IN INTERPLANETARY SPACE

By Hugh R. Anderson

Jet Propulsion Laboratory

15-1-194

## 2: PARTICLE AND FIELDS IN INTERPLANETARY SPACE

By Hugh R. Anderson

Jet Propulsion Laboratory

~~Double Code~~  
130 48 23

(JPL)  
In ~~WASH, Washington~~  
125  
Space and Planetary Environ. <sup>24</sup> Jul. 1963  
p1-15 orig (see 264-35261 09 29)

### Introduction

The entities found in interplanetary space are:

1. Planets and asteroids
2. Comets
3. Meteoroids and dust
4. Low energy photons, in particular sunlight
5. Penetrating charged particles and gamma rays
6. Low energy charged particles or plasma
7. Magnetic field

Of these, we shall be concerned chiefly with the entities in item 5. because they penetrate appreciably thick shields. It will be useful to consider item 4. for the sake of comparison, and items 6. and 7. because the plasma and associated magnetic field control the propagation of the penetrating charged particles.

### Sunlight

Sunlight consists of photons of wavelengths falling almost entirely between 2000 Å and 10,000 Å. The energy flux at a distance of 1 AU

N65 16924

from the sun is .1374 watts/cm<sup>2</sup>. The spectral distribution and intensity of light in the 2000 to 8000 Å range is approximately that which would be emitted by a black body at 5785 °K. The pressure exerted by this flux if it is fully absorbed is  $4.6 \times 10^{-5}$  dynes/cm<sup>2</sup>. The energy flux and pressure must vary as (distance to the sun)<sup>-2</sup>.

The sun emits infrared radiation out to 50,000 Å, and ultra-violet and X radiation from 1 to 2000 Å which exceeds the emission from a black body at 5785 °K. The flux of X rays is quite variable and increases when the sun is active and during solar flares. Although the radiation is not very penetrating, its effect upon surface layers of materials exposed for long periods might be significant.

#### Solar Plasma

A flux of plasma flowing outward from the sun has been hypothesized from a number of indirect observations and has been directly measured by Explorer X and most recently by Mariner II. An instrument on the latter measured the flux of positively charged particles as a function of energy per unit charge from 250 to 8300 ev/electron charge. Only positive particles that moved outward from the sun in a direction within 10° of the radial direction could be detected.

Data obtained during approximately 100 days of operation show that some positive current was always detected by the instrument. The plasma has a bulk or mean velocity and a random distribution of smaller velocities about the mean which can be characterized by a kinetic temperature. The positively charged flux must consist of protons and some alphas and heavier nuclei, although the Mariner II instrument could not identify

particle mass. Theory shows that the plasma must be electrically neutral and that the electrons move with approximately the bulk velocity. Their energy is therefore only a few electron volts. Indirect evidence suggests that the bulk velocity was nearly radial.

It was observed that the energy of the peak flux lay between 751 and 3688 ev during the operation of Mariner II. If it is assumed that only protons are observed, a typical solar plasma can be described by these parameters:

Bulk Velocity  $v_0 = 460$  km/sec corresponding to 1100 ev.

Density  $n = 2.5$  protons/cm<sup>3</sup>.

Kinetic temperature of random velocity  $T = 1.9 \times 10^5$  °K.

Thence the flux of protons was  $1.15 \times 10^8$ /cm<sup>2</sup>sec. The bulk velocity and density varied by as much as a factor of two so that fluxes as high as  $5 \times 10^8$ /cm<sup>2</sup>sec, were observed. The high velocities appear to be associated with active regions on the sun. The kinetic energy associated with the above spectrum is 2752 ev/cm<sup>3</sup>, and the impact pressure is  $8.85 \times 10^{-9}$  dyne/cm<sup>2</sup>. More detailed analysis, or the admixture of alpha particles may change the above figures a little. The velocity and density of this solar wind may also be different in different phases of the eleven-year solar activity cycle.

#### Magnetic Field

A magnetic field is imbedded in the plasma. Measurements with Mariner II show that a field is present which varies frequently by several gamma (gamma =  $10^{-5}$  gauss). It is deduced that the average field strength is of the order of 5 gamma and that the average vector lies in the plane

of the ecliptic inclined about  $45^{\circ}$  from a radial line from the sun. The instantaneous direction and magnitude of the field vary greatly from this.

The energy density of the field is about  $62 \text{ ev/cm}^3$ , which is much less than the plasma kinetic energy density. This means that the magnetic field moves with the bulk velocity of the plasma, and is dominated by its bulk motion.

Neither the plasma nor the magnetic field vary simply as (radius from the sun) $^{-2}$ . In going from the earth to the orbit of Venus at 0.724 AU, Mariner II saw no systematic change in these phenomena. Indirect evidence agrees with theory in predicting that they will retain the same characteristics for several AU beyond the earth's orbit although the flux and field intensity must decline with increasing distance.

#### Penetrating Charged Particles and Gamma Rays

The flux of electrons with energies from 1 to 40 Kev and of protons from 10 to 500 Kev has not been measured. It is probably safe to assume that the fluxes fall monotonically with increasing energy in these intervals.

Particles with greater energy belong to either a steady component or to the sporadic, solar cosmic ray component. The kinetic energy density of these particles is much less than the field energy density so that motion of the particles is determined by the magnetic field associated with the plasma. The steady component consists of the galactic cosmic ray flux and possibly of some particles produced in the sun in such a way that their flux at the earth is constant and isotropic. The galactic cosmic ray flux is assumed to be constant and isotropic outside of the solar system, but the

amount which reaches the earth depends upon the interplanetary magnetic field, the solar plasma, and thence upon solar activity. Changing solar activity produces variations of a few percent with time scales of a few days. The eleven-year cycle of solar activity produces a corresponding cycle of galactic cosmic ray flux at the earth with the feature that when solar activity is high, the cosmic ray flux is low. The fractional change of flux depends upon energy, and amounts to more than a factor of two in particles in the 150 to 500 Mev range.

The flux of particles with energy greater than 10 Bev per nucleon is constant and isotropic within a few percent. The flux of protons is  $J_p(>10 \text{ Bev}) = 2 \times 10^{-2} \text{ protons/cm}^2\text{sec sterad}$ . Figure 1 shows an integral energy spectrum of particles with energy above 1 Bev. The composition of this flux may be expressed as the relative abundance of different nuclei above a constant kinetic energy per nucleon and is

94% protons  
5.5% alphas  
0.5% heavier nuclei.

The relative abundance above a constant magnetic rigidity is

86% protons  
13% alphas  
1-2% heavier nuclei

The numbers above a constant rigidity are approximately independent of rigidity at both relativistic and non-relativistic energies. The rigidity description is therefore preferred.

Between 0.150 and 10 Bev per nucleon, the composition above a constant rigidity is the same as that at the higher energies, and so far as has been determined, is independent of rigidity and solar activity. The flux varies inversely with solar activity in an eleven-year cycle so that  $J_p(>150 \text{ Mev}) = 0.1 \text{ to } 0.25/\text{cm}^2\text{sec sterad}$ . Figure 2 shows the integral energy spectrum of protons in this range in 1956 and 1958-59. The ionization rate due to these particles varies from 1 to 2.5 millirads per hour, which amounts to 8 to 20 rads per year, approximately.

The flux of particles between 10 and 150 Mev is not known except for the years 1960-62. At this time, which is midway between the solar maximum in 1957-58 and the next minimum in 1965, the flux of protons with energies between 10 and 150 Mev was  $\approx 0.01/\text{cm}^2\text{sec sterad}$ . These particles may be galactic cosmic rays or may originate in the sun. If the former is the case, their flux will increase as solar activity declines. If they originate in the sun, their flux is expected to decrease with declining solar activity and increase when the sun becomes more active.

Instruments on Mariner II in 1962 measured the average omnidirectional flux and the rate of ionization of particles behind  $0.2\text{g}/\text{cm}^2$  of shielding. This shield passes protons with  $E > 10 \text{ Mev}$  and electrons with  $E > 0.5 \text{ Mev}$ . Figure 3 shows data obtained up to the time of encounter. The omni-directional flux of  $3.0/\text{cm}^2\text{sec}$ , corresponds to an unidirectional flux of  $0.24/\text{cm}^2\text{sec sterad}$ , while the rate of ionization corresponds to a dose rate of about 1 millirad per hour.

The measured flux does not vary systematically with distance

from the sun. This and other considerations make it seem likely that at any given time the cosmic ray flux is uniform throughout the volume between 0.5 and 5.0 AU from the sun. However, this has not yet been proved.

### Solar Cosmic Rays

Following a few solar flares, protons and heavier nuclei reach the earth in large numbers and are observed for a few hours or days thereafter. The particles are evidently injected into interplanetary space by the sun at the time of the flare. They are then trapped within a large volume by the interplanetary magnetic field, and slowly diffuse into interstellar space. The flux at a fixed location therefore builds up rapidly and then decays. The energy spectrum and time history are different in each case, but in general the energy spectrum falls more steeply with energy than that of the galactic cosmic rays. Figure 2 shows integral spectra measured in two events. The higher energy particles arrive at the earth first following the flare, and decay away faster than the lower energy particles. Thus the energy spectrum becomes steeper with time.

Figure 4 shows the radiation behind  $0.2\text{g/cm}^2$  ( $E_{\text{proton}} > 10 \text{ Mev}$ ) measured by Mariner II on 23-24 October 1962. The time history has a typical rapid rise and slow decay. In many events, the flux of particles of a single energy varies exponentially with time. Peak fluxes of protons above 30 Mev range on different occasions from 0 to at least  $4 \times 10^3$  protons/cm<sup>2</sup>sec sterad. Protons predominate, but proton/alpha ratios between 30:1 and 1:1 have been detected. There are a few percent of electrons,

and the ratio alpha/heavier nuclei ranges from 42:1 to 100:1.

The connection between flux, time history and solar activity is not unique, but the following correlations have been established:

- A. The peak flux is roughly proportional to the size of the optical flare.
- B. A flare must be on the visible disc to produce particles that reach the earth. The western half of the disc is preferred, and western hemisphere flares are more likely to produce direct radiation than are eastern ones.
- C. Flares which produce cosmic rays usually emit broad band radio noise (Type IV noise) in the 7-100 megacycle range.
- D. Flares which produce particles usually occur in well developed active regions on the sun.

The previously existing interplanetary magnetic field determines the propagation of particles from the sun to the earth.

- E. Direct radiation reaches the earth if the interplanetary field is ordered. This could be the case if the active region had been ejecting solar plasma for several days before the flare occurred.
- F. Only indirect radiation can reach the earth if there is no ordered connection between the sun and earth.

When the direct radiation reaches earth it is anisotropic so that it appears to come from a small source located within  $50^{\circ}$  of the sun. The flux reaches the earth 5 to 10 minutes after the flare and attains a maximum within 5 to 20 minutes. Relativistic protons decay with a time constant the order of one hour, while the slower protons require several hours.

Indirect radiation, which is isotropic, always accompanies direct radiation. The indirect radiation arrives 10-60 minutes after the flare, and rises to a peak within 1 to 3 hours; the rise time is 4 to 10 times the delay time. The decay time is of the order of 4 to 12 hours, and is roughly proportional to the rise time.

In more than half the cases, only indirect radiation is observed. The relativistic radiation first arrives at the earth 1 to 3 hours after the flare in these cases and the slower particles can be delayed up to 6 hours. This represents the longest observed delay time between the flare and the arrival of radiation. The flux rises to a peak in 4 to 30 hours, which is 4 to 10 times the delay time. The characteristic decay time lies between 4 to 60 hours and is again approximately proportional to the rise time.

#### Frequency of Occurrence of Solar Cosmic Rays

The incidence of solar cosmic ray events has been discussed in the Solar Proton Manual, (Solar Proton Manual, edited by F. B. McDonald, Goddard Space Flight Center, 1963. Report #X-611-62-122), and the data in this section are from that source.

In the years 1956-1961, the largest flux of solar cosmic rays was observed on 23 February 1956. The flux of protons with  $E > 30$  Mev is estimated to have been  $4 \times 10^3/\text{cm}^2\text{sec sterad}$  producing a dose of 50 rads/hour. The total dose in the event was 2000 rads from protons with  $E > 30$  Mev, (Range =  $1.16\text{g}/\text{cm}^2$  of Al) and 80 rads from protons with  $E > 100$  Mev, (Range =  $9.85\text{g}/\text{cm}^2$  of Al). Although these values are somewhat uncertain because of the experimental techniques used at that date, the 23 February event is undoubtedly the largest in the years studied. The next highest dose rate was 20 rads/hour.

Figure 5 shows the total dose in each of the larger events in the years 1956-1961 due to protons with  $E > 30$  Mev (top of bar) and  $E > 100$  Mev (triangular mark on each bar). The yearly dose from galactic cosmic rays with  $E > 150$  Mev/nucleon is shown also.

In several cases a single active solar region produced several flares and cosmic ray outbursts within a few days. The following table of events can be constructed from Figure 5 and a table of solar activity.

Table I

Incidence of Solar Cosmic Ray Events

Dose produced by protons with $E > 30$ Mev in each event:	Number of Events:	Number of active regions:	
$> 800$ rads	2 events	in	2 regions
$> 400$ rads	6 events	in	4 regions
$> 200$ rads	6 events	in	4 regions
$> 100$ rads	9 events	in	6 regions
$> 50$ rads	12 events	in	9 regions

The very large outbursts ( $>200$  rads each) were produced by 4 regions each active for a week or less. The average dose due to all other events in the six-year period was 67 rads/year, with the highest dose in a single year being 240 rads in 1958. It should be noted that the doses due to protons with  $E > 100$  Mev were more than an order of magnitude less than these values. The effect of secondary particles has not been taken into account in making these estimates.

### Conclusion

The large solar cosmic ray events are the only radiation in interplanetary space which is known to be hazardous to man. In the years 1956-1961, active regions which produced such outbursts appeared on the average of once every eighteen months. This frequency is consistent with all earlier observations of events. There is a tendency for large events to occur more frequently when solar activity is increasing or declining than at the maximum or minimum of activity. The only way to improve our knowledge of the frequency of these events is to observe more of them.

Radiation reaches the earth no later than 3 hours after the flare and is usually delayed less than an hour. However, up to an hour's exposure to the most intense fluxes observed would not be fatal.

Large outbursts are generated in well developed active regions on the sun. It has been suggested that hazardous and safe intervals of a few days can be predicted one or two weeks in advance by observing the size of sunspot penumbra in active regions. (Kinsey Anderson, University

of California, Preliminary Study of Prediction Aspects of Solar Cosmic Ray Events, NASA Technical Note D-700, dated April 1961.) No method is known to predict large flares many weeks or months in advance.

# INTEGRAL ENERGY SPECTRUM OF GALACTIC COSMIC RAYS

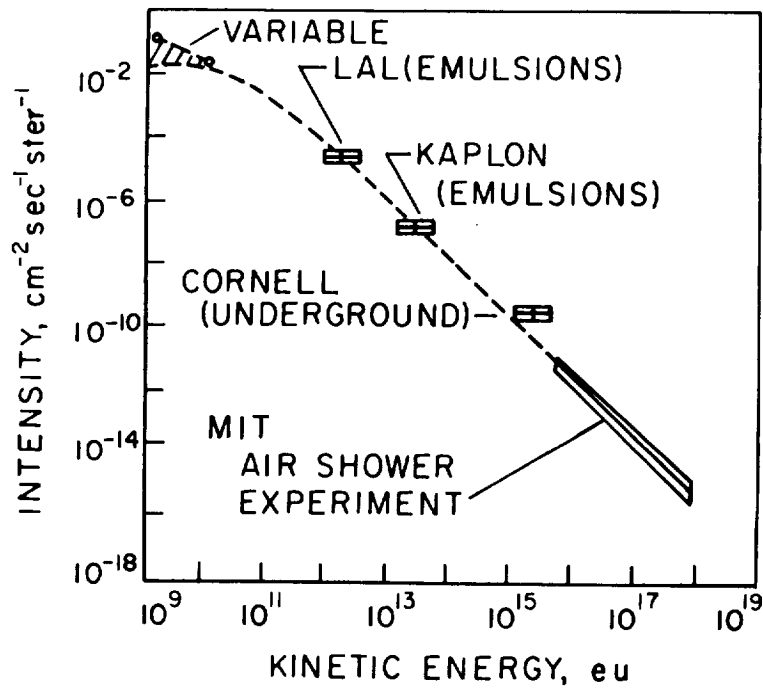


Figure 1

## INTEGRAL ENERGY SPECTRA OF COSMIC RAY PROTONS IN 1956 AND 1958-59, AND OF SOLAR COSMIC RAY PROTONS DURING TWO EVENTS

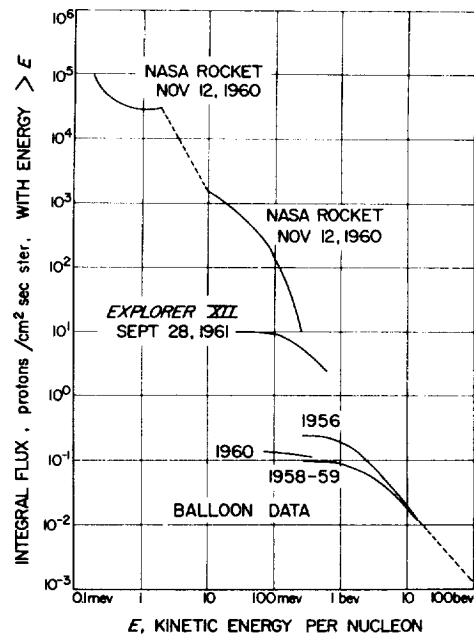


Figure 2

# RADIATION MEASURED BY MARINER II BEHIND $0.2\text{G}/\text{CM}^2$ OF STEEL. THE CUTOFF FOR PROTONS IS 10 MEV

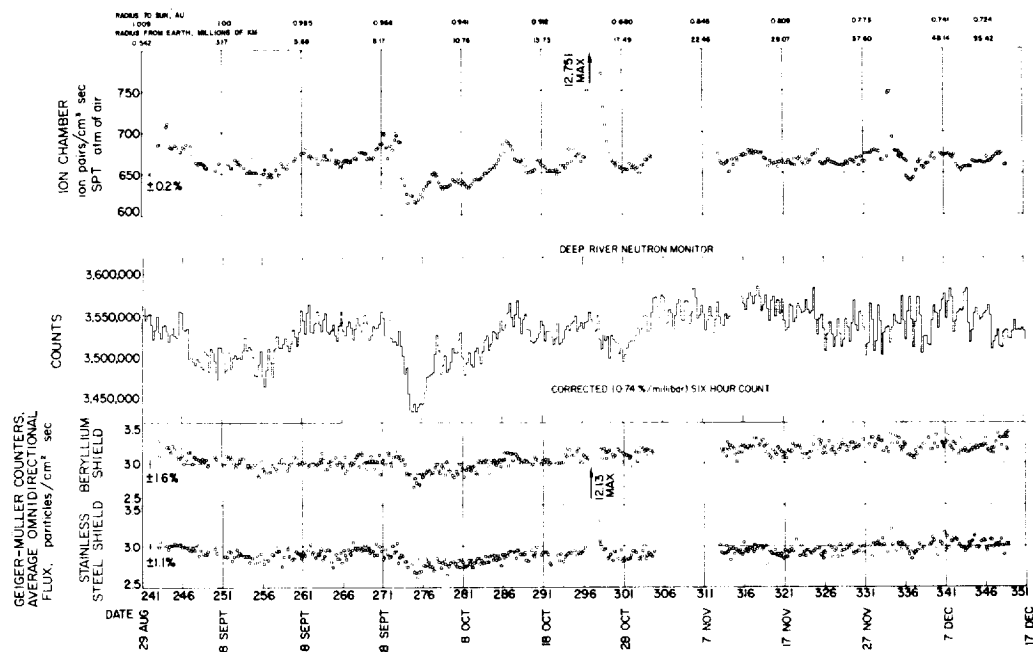


Figure 3

## RADIATION MEASURED BY MARINER II BEHIND $0.2\text{G}/\text{CM}^2$ OF STEEL DURING A SMALL SOLAR COSMIC RAY EVENT ON 23-24 OCTOBER 1962

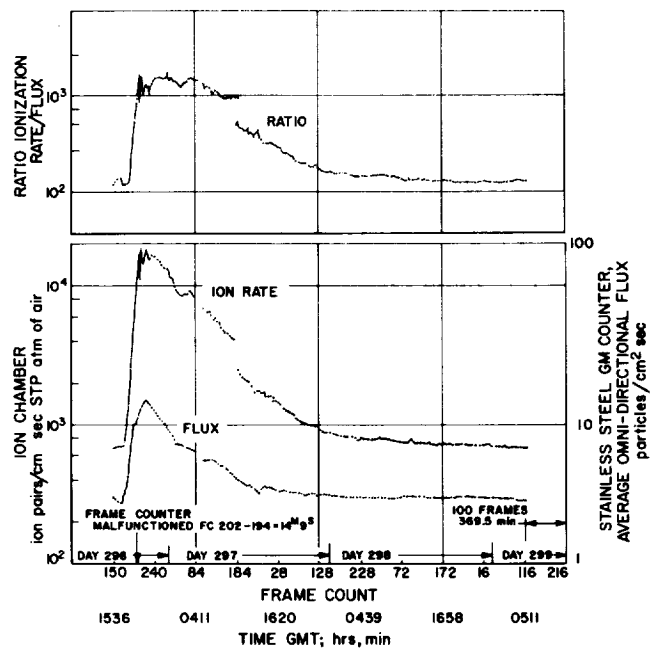


Figure 4

DOSE RESULTING FROM PROTONS WITH  $E > 30$  MEV (TOPS OF BARS) AND  $E > 100$  MEV (TRIANGLES) IN THE PRINCIPAL SOLAR COSMIC RAY EVENTS DURING 1956-1961. THE YEARLY DOSE FROM GALACTIC COSMIC RAYS WITH  $E > 150$  MEV/NUCLEON IS ALSO SHOWN

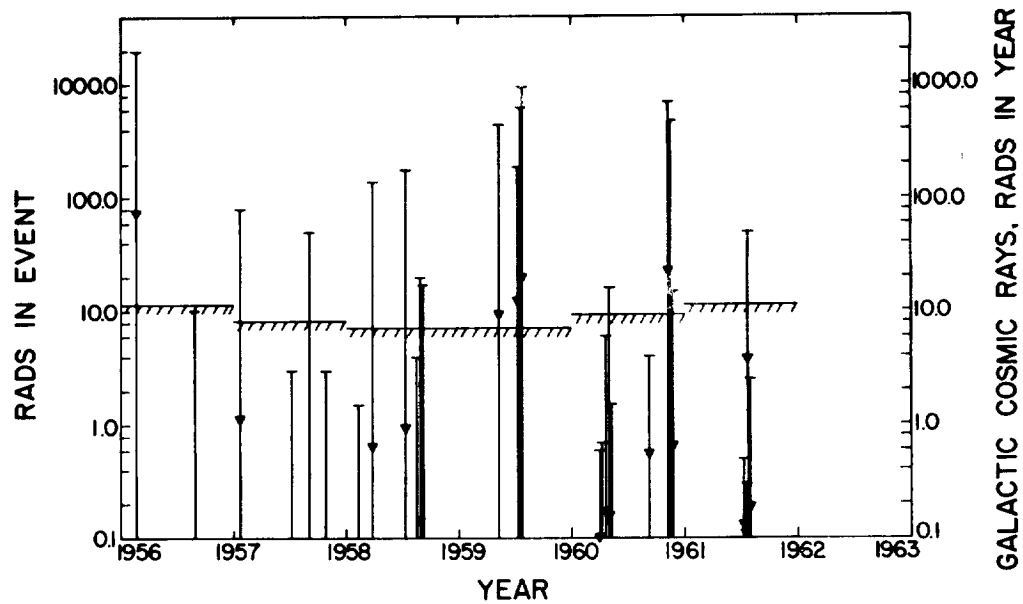


Figure 5



METEOROID HAZARDS IN NEAR EARTH AND DEEP SPACE

By C. T. D'Aiutolo

NASA Headquarters

1165-16725



6; METEOROID HAZARDS IN NEAR EARTH AND DEEP SPACE

By C. T. D'Aiutolo

*In its Space and*

NASA Headquarters

*Washington, D.C.*

*Planetary Environ. Jul. 1963 p 19-31 refs (see*

ABSTRACT

*x64-35261 02 29}*

*16925*

Although the meteoroid hazard has not been adequately evaluated for proper design of spacecraft for near-earth, cislunar, as well as interplanetary space missions, the extent of meteoritic encounters on space exploration may be estimated. The available information about meteoroids and cosmic dust obtained from ground-based observations and satellite measurements, with particular emphasis on the results of the Explorer XVI, is used to estimate the distribution of meteoroids near the earth and in interplanetary space. An estimate of the hazard has been made using appropriate hypervelocity cratering criteria. It is shown that based, on current results, the penetration hazard due to sporadic meteoroids in interplanetary space is expected to differ little from that near-earth. However, for long missions, near the earth, it will be necessary to design optical surfaces and thermal coatings with due regard to the dust belt encompassing the earth. The effects of meteoroid showers and asteroids are briefly discussed and it is concluded that considerable more research is required before spacecraft can be properly designed to fulfill their missions in near-earth as well as interplanetary space environments.

INTRODUCTION

*Author*

The effects of meteoritic encounters on space vehicles are a matter of concern in the design of spacecraft for various near-earth, cislunar, and interplanetary missions. The hazard from meteoroid impacts may be evaluated from knowledge of the distribution of interplanetary matter in the solar system and knowledge of the characteristics of cratering and penetration from meteoroid impacts on spacecraft structures. Various estimates of the hazard have been made using data derived from visual, radio, and optical observations of meteors, and from direct measurements using probes and satellites together with hypervelocity penetration criteria based either upon laboratory results or theoretical models. Typical of these estimates are shown on figure 1. Shown is a log-log plot of the estimate number of penetrations per square foot per day as a function of the thickness of aluminum sheet in inches. The upper curve combines the distribution of meteoroids as proposed by Whipple in 1957, reference 1, with the Charters and Summers penetration criteria, reference 2, while

the bottom curve combines the distribution proposed by Watson, reference 3, in 1941 with the Bjork penetration criteria, reference 4. The large spread in the curves results from the estimates of the mass of a zero magnitude meteor and the dependency of meteoroid velocity on the depth of penetration. There is no discrepancy in the influx of meteoroids since both authors based their measurements on the same observations. However, Watson estimated a zero magnitude meteor as having a mass of 0.25 grams and a velocity of 55 km/sec. and assumed an average meteoroid density of about 3 gms/cm<sup>3</sup>. Whipple on the other hand estimated a zero magnitude meteor as having a mass of 25 grams and a velocity of 28 km/sec. He assumed an average meteoroid density of about 0.05 gm/cm<sup>3</sup>.

Charters and Summers penetration criteria, based on laboratory hypervelocity impact investigations states that the depth of penetration is proportional to the impact velocity to the 2/3 power, while Bjork's criteria based on theoretical hydrodynamic model states that penetration depth is proportional to the velocity to the 1/3 power. As may be seen there is over three orders of magnitude spread between the estimates.

Admittedly these estimates are considerably greater than some others that have been proposed, however they illustrate the point that a great uncertainty exists in predicting the meteoroid hazard to spacecraft.

#### RECENT DIRECT MEASUREMENTS

Recently a spacecraft has been placed in a near-earth orbit to obtain a direct measure of the penetration rates from meteoroids in thin structural materials with the viewpoint of narrowing the uncertainty illustrated by the curves shown on the first slide.

This spacecraft, the Meteoroid Satellite S-55b, designated Explorer XVI (1962 Beta Chi) is providing useful data on penetration rates. In fact, definitive penetration data have been obtained for the first time by this spacecraft. Figure 2 is a photograph of the Explorer XVI. It is about 76 inches long, about 23 inches in diameter and is installed around the last stage (X-248 rocket motor) of the Scout launch vehicle. Time does not permit a complete description of the spacecraft but of interest here is that the spacecraft contains five experiments to record meteoroid encounters. All experiments are mounted around the periphery of the spacecraft. A schematic drawing of the spacecraft is shown figure 3. Mounted on the forward section are cadmium sulfide cell detectors (two - 180° apart) as well as impact detectors located under "sounding boards." These impact detectors have sensitivities corresponding to two momentum levels. Aft on the main body of the spacecraft are 160 pressurized cell detectors (skins thicknesses of 1, 2, and 5 mils) which are described below. Aft

of the cells are 60 grid detectors bonded beneath thin stainless steel skins, (thicknesses: 1, 3, and 6 mils) and below these detectors are 46 wire card detectors composed of a thin winding of copper wire (two and three mils in thickness).

The spacecraft is a cooperative effort of three NASA Research Centers. Project management as well as overall systems responsibility is at Langley with experiments being provided by Langley, Lewis and Goddard. The grid detector experiment was developed at the Lewis Research Center and Elmer Davison is the experimenter. The wire card as well as the cadmium sulfide cell experiments were developed at Goddard and Luc Secretan is the experimenter. The pressurized cell and the impacting detecting experiments were developed at Langley. Al Beswick is the impact detector experimenter, and Charles Gurtler is the pressurized cell experimenter.

The pressurized cell detector, is the primary experiment. Figure 4 is a drawing of the cell. A total of 160 annealed beryllium-copper cells are mounted around the periphery of the rocket motor case in 5 rows of 32 cells each. Each cell is filled with helium. When the cell is punctured, the gas leaks out and the pressure loss actuates a switch that signals the telemeter of the puncture. Thus, after one puncture, the cell cannot indicate additional punctures.

The Explorer XVI was placed into orbit from Wallops Island by means of a Scout launch vehicle on December 16, 1962. It is performing as designed and all indications are that a long useful life is expected. Several penetrations have been recorded. Shown in figure 5 is the accumulated punctures received in the pressurized cells from launch thru April 18, 1963. During the four months in orbit, 33 one-mil Be-Cu penetrations and 9 two-mil Be-Cu penetrations have been recorded. No five-mil Be-Cu cells have been penetrated in this time period. Although not shown, several penetrations have occurred in the Cd-S cell experiment and three penetrations in the one-mil stainless steel grid experiment. No penetrations have been received in the two-and-three-mil copper wire cards nor in the three-and-six-mil stainless steel grid experiments. Several hundred impacts have been recorded but as yet these data are not completely analyzed.

Tests were conducted at Langley to ascertain a correlation of penetration depth in Be-Cu and one of the more common structural materials such as aluminum. Figure 6 presents the results of this test. One-sixteenth inch aluminum projectiles were fired into quasi-infinite aluminum and beryllium-copper targets to velocities of about 17,000 feet per second. From these data it appears that the penetration depth in aluminum is about twice that in beryllium-copper.

Using these results penetration rates received in the Be-Cu cells are plotted at the corresponding thickness of aluminum in figure 7. Shown are the number of penetrations per square foot per day for the

one-mil and two-mil Be-Cu cells plotted at two-and-four-mils of aluminum, respectively. It is noted that the rates plotted include an earth shielding factor so that they may be compared to the estimates shown. Error bars on the points are the 95% confidence limits.

Although no penetrations have been received in the five-mil Be-Cu cells an upper estimate of the penetration rate can be made. This upper value is shown plotted at a value of 10 mils of aluminum in the figure, for 95% confidence. Also plotted is the 50% probability point for the expected penetration rate. It is clear from these data that the Whipple distribution combined with the Charters and Summers penetration criteria greatly overestimates the meteoroid hazard in thin materials, while the Watson-Bjork estimate is slightly below the actual measured data.

On the basis of the Explorer XVI data it appears that the Whipple-Charter'-Summers' estimate of the hazard if used would result in the weight required for protection from meteoroids that would be excessive.

The Explorer XVI data do not in themselves clearly define the expected penetration rates over a wide range of material thicknesses; however, the use of these data together with ground observations will allow a more realistic estimate of the expected hazard.

#### AVERAGE EXPECTED METEOROID IMPACTS

Presented in figure 8 are cumulative meteoroid impact rates as a function of mass as determined from several observations and direct measurements by probes and satellites. Shown are the Whipple (1957), Watson (1941), as well as the Whipple (1963), reference 5 estimates based on optical measurements of meteors. Also shown is the Watson (1941) estimate revised by Whipple in 1963, reference 5. The curves labeled V. d. Hulst (1947), reference 6, and Ingham (1961), reference 7, are based on Zodiacal light measurements. Direct measurements are shown by the curves labeled Alexander et al, reference 8, and Soberman and Heminway, reference 9, as well as the data points labeled Pioneer I, reference 10, and Mariner II, reference 11. The Explorer XVI data points were determined from the previously presented data thru the use of the Bjork penetration criteria. All data presented on this slide assume a mean meteoroid density of  $0.44 \text{ gms/cm}^3$  and a mean velocity of 30 km/sec. which is consistent with the analysis by Whipple (1963) of optical meteor observations.

The measurements by McCracken et al were made near earth, while the Pioneer I data were obtained to distances of about 20 earth radii. The Mariner II data were obtained over distances from the earth to the vicinity of Venus. From these data it is immediately apparent that the impact rates based on direct measurements decrease as the distance from the earth increases from which it can be inferred that there is indeed

a dust belt about the earth. Also there is good agreement between the revised Watson curve and an interpretation of the dust content in the Zodiacal cloud. A most interesting result is shown in the agreement in the flux of particles capable of penetrating thin metallic skins (Explorer XVI data) and the Zodiacal light curve (Ingham 1961). The Whipple 1963 curve is based on the Hawkins-Upton influx rate, reference 12, and extrapolates these data to smaller meteoritic masses ( $m \sim 10^{-3}$  gms). There is no evidence to indicate that influx of small meteoroids will follow the same distribution as the mass of larger ones.

Therefore based on the data presented there is no real discrepancy between the ground observations and we may expect that the true interplanetary meteoroid density at one astronomical unit to be along a curve composing the Ingham (1961) curve and the revised Watson curve, illustrated in figure 9. However near the earth the density of meteoroids may be 3-6 orders of magnitude greater than the interplanetary density as indicated by the direct measurements of McCracken et al and Soberman and Heminway.

There is a great discrepancy (about 4 orders of magnitude) between the Explorer XVI data and the data of McCracken et al. These direct measurements were made near the earth and indicate that although the earth is encompassed by a dust belt of relatively high density as compared to interplanetary space only a small percentage of these meteoritic particles are able to penetrate thin metallic skins.

Based on the data presented in the previous slide a variation of the average number of meteoritic impacts with meteoritic mass is suggested and is shown in figure 10.

For missions to deep space the lower curve may be used as an estimate of the average number of meteoritic encounters of a given mass on larger, while for missions near the earth the upper curve may be used. The number of encounters may increase by a factor of 5 to 10 during periods of recognizable sporadic showers and several of the known meteor showers.

#### PENETRATION FROM METEOROID IMPACTS

As pointed out earlier in this paper, in addition to a knowledge of the number of meteoritic encounters to be expected, it is necessary to establish the characteristics of impact cratering and penetration from meteoroid impacts on spacecraft structures in order to estimate the meteoroid hazard.

It is unfortunate that the current limitations of hypervelocity impact facilities is in the velocity region where it is difficult to say from an extrapolation of the data whether penetration depth is dependent on the velocity to the  $1/3$  or  $2/3$  power. Shown in figure 11 is a typical variation of penetration depth (normalized to projectile

diameter) with velocity. In addition to the experimental data, curves showing dependency of penetration depth with velocity are presented. As pointed out previously the Charters and Summers curve states that the depth varies as velocity to the  $2/3$  power, while the Bjork curve states that depth varies as velocity to the  $1/3$  power.

The Charters and Summers criteria is based on experimental data obtained at relatively low velocities and extrapolated to meteoritic velocities. Bjork's criteria is a theoretical one based on a hydrodynamical model. Although it is not conclusive, the Bjork criteria is the preferred one since his theoretical approach is considered to be a good representation of the actual cratering process.

Combining the average number of meteoritic encounters with the Bjork penetration criteria allows a realistic estimate of the meteoroid hazard. This estimate is shown in figure 12. The curve here may be used to estimate the average expected number of penetrations in aluminum near the earth as well as in interplanetary space. This curve represents a good estimate for long time missions; however, for short exposure times during known or sporadic meteor showers the expected penetration rates shown may be too low by a factor of 5 to 10. At radial distances from the sun between 1.5 and 5 astronomical units (in the vicinity of Mars) the collision hazard from asteroidal debris may be greater than that shown. At this time it is not known how much greater the expected hazard may be.

The curve shown combines the ground observations of meteors and Zodiacal Light measurements with the Bjork penetration criteria. Comparison of the direct measurements made near the earth indicate that there is about four orders of magnitude difference between the number of meteoritic encounters and the number of particles capable of penetrating thin metallic skins. On this basis it is suggested that the curve presented to be used as an estimate of the expected penetration rates near the earth as well as in interplanetary space.

For long exposure time near-earth missions however, due consideration must be given to the adverse effects of the dust belt encompassing the earth on optical surfaces and thermal coatings.

### CONCLUSIONS

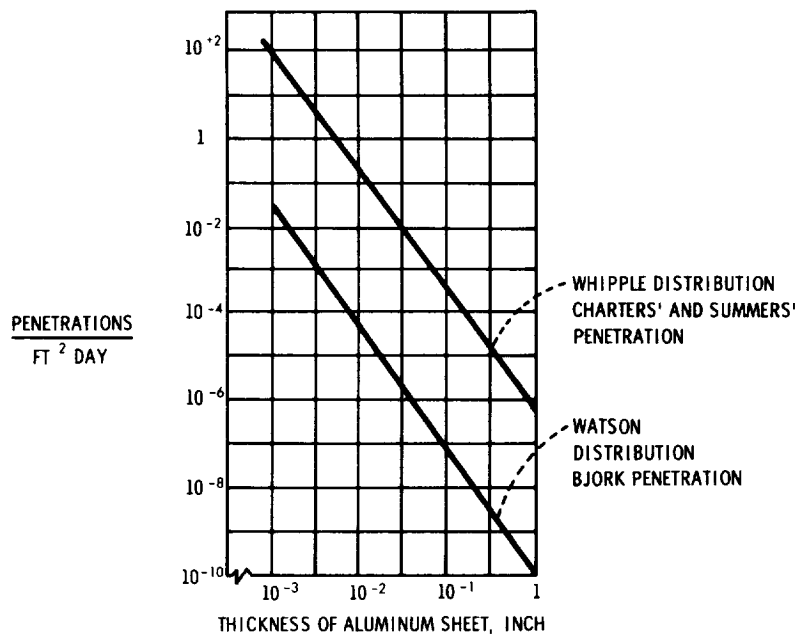
An attempt has been made using current measurements to reappraise the meteoroid hazard to spacecraft. This reappraisal is at best an estimate since it is based on a number of assumptions. In order to more accurately determine the meteoroid hazard considerable research is required in determining the characteristics of meteoritic particles over the size spectrum. In addition the characteristics of impact cratering and penetration at meteoritic velocities by particles simulating meteoroids must be determined. Further, more definitive direct measurements are required in the space environment.

NASA has established a borad Meteoroid Technology Program to provide these required data. The program is a long range one and is designed to provide gross answers at an early data and more refined data, should they be required, at a later time. In this manner the meteoroid hazard to spacecraft can be properly evaluated on a timely basis.

#### REFERENCES

1. F. L. Whipple, Vistas in Astronautics, Vol I (M. Alperin, ed) Peramon Press, London 1958.
2. J. L. Summers, Investigation of High-Speed Impact: Regions of Impact and Impact at Oblique Angles, NASA Technical Note D-94 (1959).
3. F. G. Watson, Between the Planets, Harvard University Press, Cambridge (1956).
4. B. L. Bjork, Meteoroids vs Space Vehicles, American Rocket Society Journal 31 (1961) 803.
5. F. L. Whipple, on Meteoroids and Penetration Ninth Annual American Astronautical Society Meeting, Los Angeles, California. (1963).
6. H. C. van de Hulst, Astrophysical Journal 105 (1947) 471.
7. M. F. Ingham, Monthly Notices Royal Astr. Soc. 122 (1961) 157.
8. W. M. Alexander, C. W. McCracken, L. Secretan, and O. E. Berg, Review of Direct Measurements of Interplanetary Dust from Satellites and Probes Space Research, Vol III (to be published) 1961.
9. R. S. Soberman, C. L. Heminway, et al., Micrometeorite Collection from a Recoverable Sounding Rocket, (A Series of Three Papers), Geophysics Research Directorate Research Note No. 71, AFCRL, Bedford, Mass. 1961.
10. M. Dubin, Proceedings of the First International Space Science Symposium, Nice, January 1960, Page 1092. Ed. H. K. Kallman - Bijl, Amsterdam: North-Holland Publishing Company
11. W. M. Alexander, Cosmic Dust, Science 138, 7 December 1098

## ESTIMATED METEOROID HAZARD



NASA RV 63 - 1381

Figure 1

## EXPLORER XVI

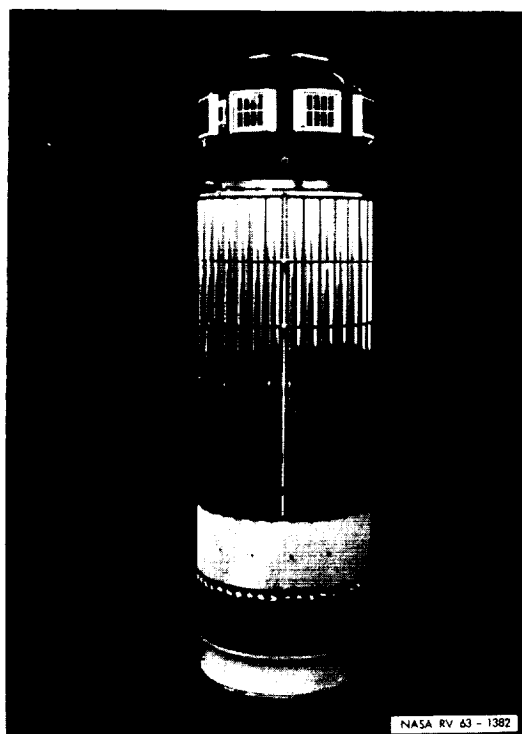
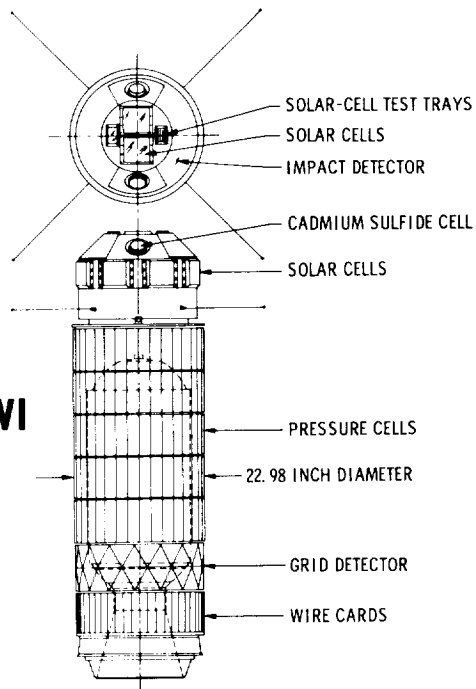


Figure 2

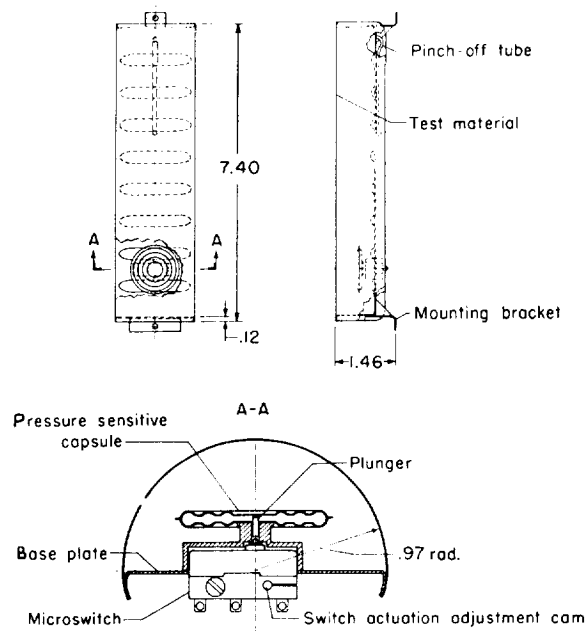
## EXPLORER XVI



NASA RV 63 - 1383

Figure 3

## EXPLORER XVI PRESSURIZED CELL EXPERIMENT



NASA RV 63 - 1384

Figure 4

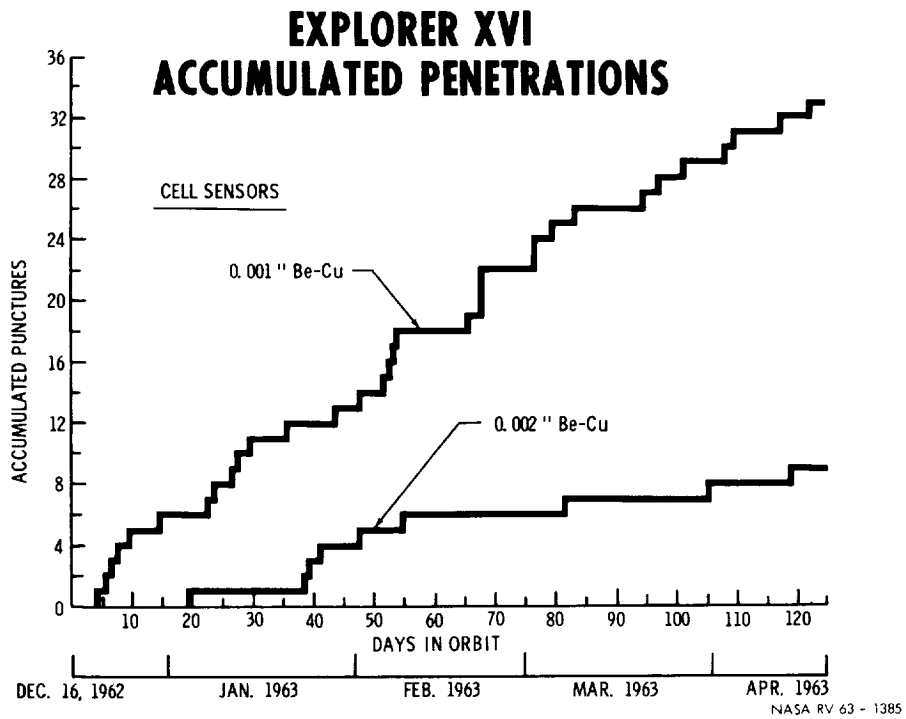


Figure 5

## PENETRATION DEPTH CORRELATION

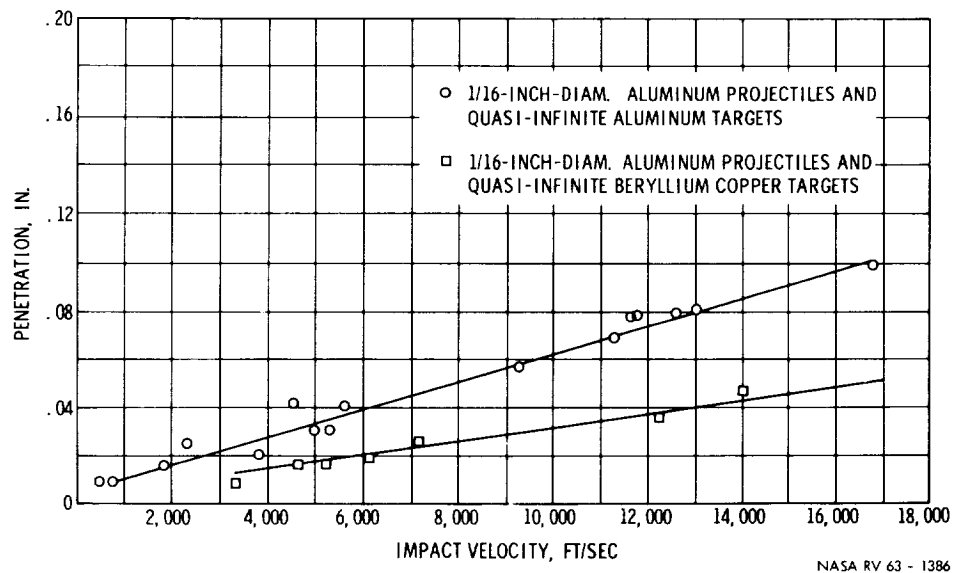
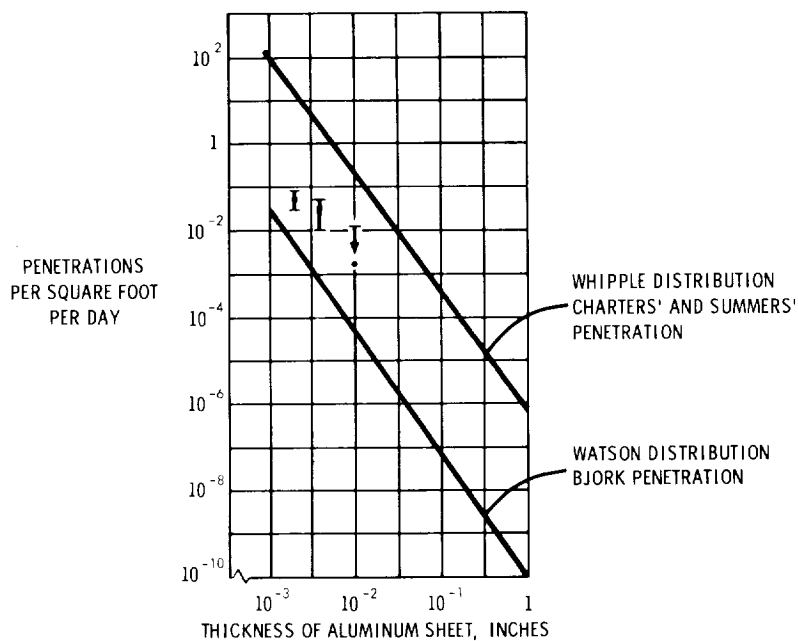


Figure 6

## EXPLORER XVI PENETRATION RATES



NASA RV 63 - 1387

Figure 7

## CUMULATIVE METEOROID IMPACT RATES

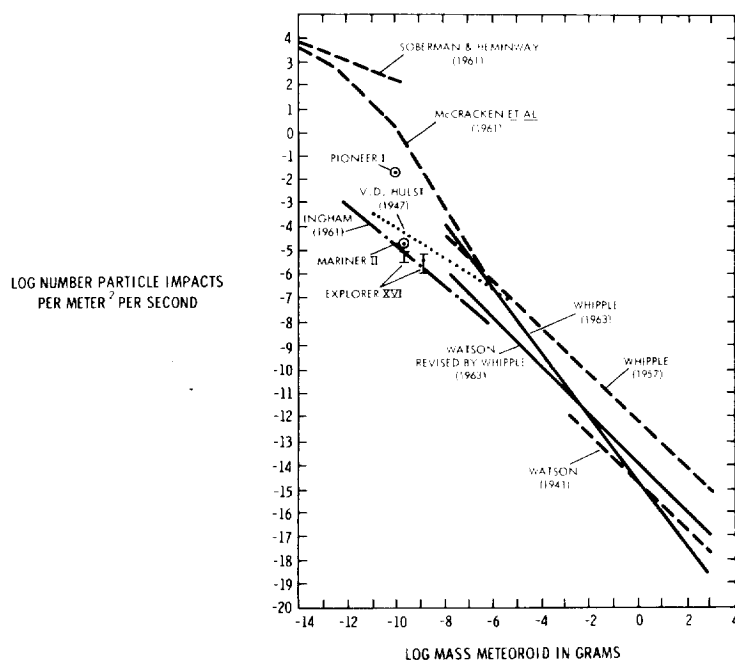


Figure 8

# INTERPLANETARY METEOROID DENSITY

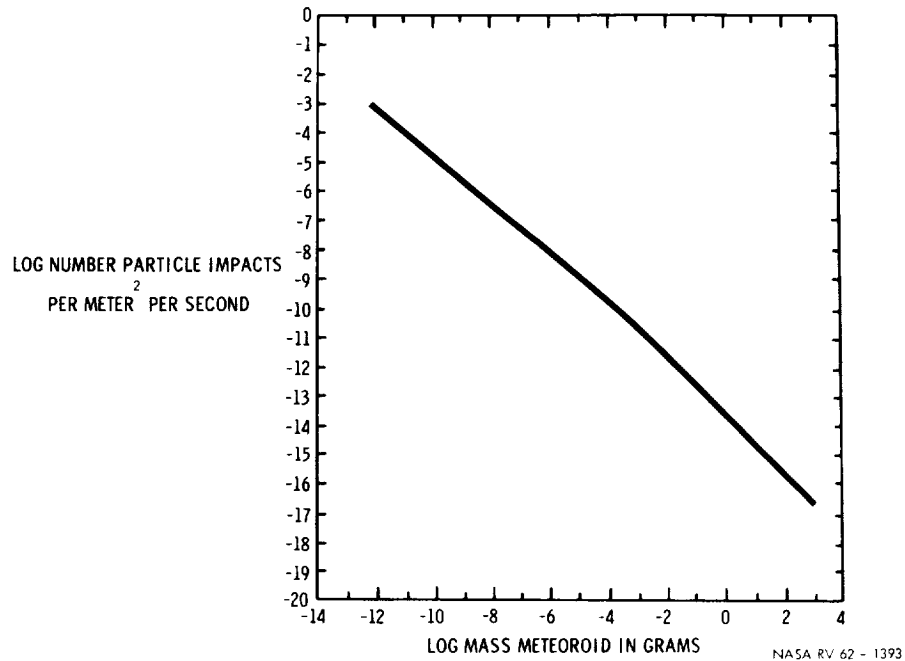


Figure 9

## AVERAGE CUMULATIVE METEOROID IMPACT RATES

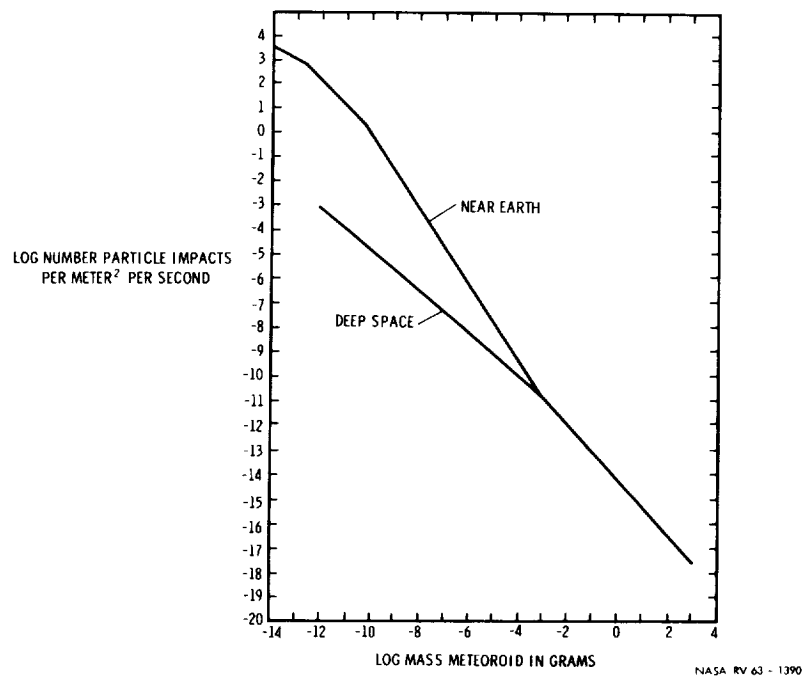
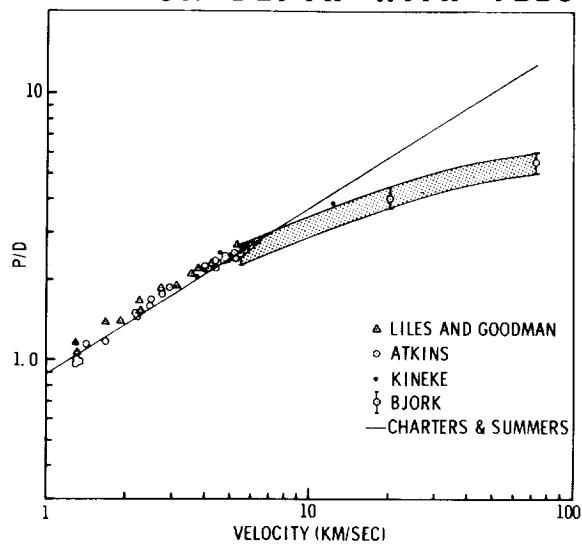


Figure 10

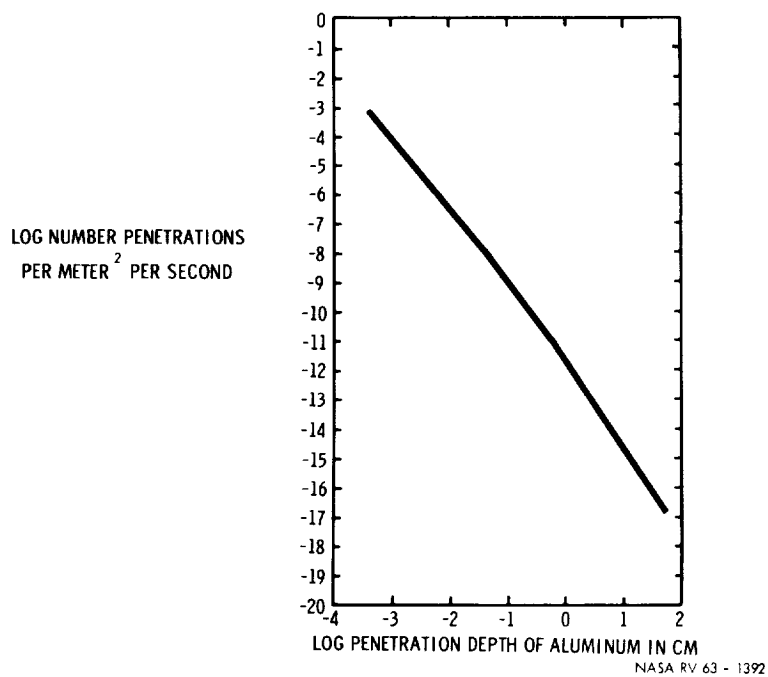
## TYPICAL VARIATION OF PENETRATION DEPTH WITH VELOCITY



NASA RV 63 - 1391

Figure 11

## ESTIMATED RATES OF PENETRATION



NASA RV 63 - 1392

Figure 12